A Letters Journal Exploring the Frontiers of Physics

February 2010

EPL, **89** (2010) 39002
doi: 10.1209/0295-5075/89/39002

www.epljournal.org

Tachyonic spectral fits of γ-ray bursts

R. Tomaschitz[(a)]

Department of Physics, Hiroshima University - 1-3-1 Kagami-yama, Higashi-Hiroshima 739-8526, Japan

received 2 December 2009; accepted in final form 14 January 2010
published online 17 February 2010

PACS 98.70.Rz – γ-ray sources; γ-ray bursts
PACS 52.27.Ny – Relativistic plasmas
PACS 95.30.Gv – Radiation mechanisms; polarization

Abstract – Evidence for superluminal radiation in γ-ray burst (GRB) spectra is pointed out. The spectral maps of GRB 941017, GRB 990123, and GRB 990104 are analyzed. The superluminal radiation modes are generated by the shock-heated ultra-relativistic source plasma. The tachyonic radiation field is a real Proca field with negative mass-square, coupled to the electron gas by a frequency-dependent fine-structure constant. At GeV energies, the coupling constant approaches a limit value, so that the radiation field is minimally coupled to the electron current. In the soft γ-ray band, the interaction with the GRB plasma becomes nonlocal, due to the varying coupling strength depending on the energy of the radiated modes. The spectral fitting with tachyonic flux densities generated by nonlocal plasma currents is explained. Estimates of the tachyonic luminosity, temperature, and internal energy of the electronic source plasma are obtained from the spectral fits.

Introduction. – γ-ray burst spectra [1–5] are scrutinized in search for superluminal radiation modes, by performing tachyonic spectral fits to the γ-ray bursts GRB 941017, GRB 990123, and GRB 990104. Tachyonic flux densities have shown to be efficient in reproducing GeV and TeV spectra of Galactic sources such as supernova remnants and of active galactic nuclei [6]. Here, we study lower energies, burst spectra in the 30 keV–100 MeV range. In this energy band, we have to take into account the frequency dependence of the tachyonic fine-structure constant $\alpha_{\rm q}(\omega)$, by which the tachyonic radiation field couples to the shocked source plasma. At GeV energies, $\alpha_{\rm q}(\omega)$ attains a limit value, so that the radiation field is coupled to the electron current by minimal substitution [7]. In the soft–γ-ray band, the energy-dependent fine-structure constant results in a nonlocal interaction of the radiation modes with the electron plasma. The goal is to quantify this interaction by way of spectral fits. This is possible since the varying coupling strength is manifested in the measured flux density of the GRBs as well as in the burst duration.

We study the long-range dispersion caused by this nonlocal coupling of tachyonic radiation modes to the electron current, and analyze the effect of the frequency-dependent fine-structure constant on the spectral functions of an ultra-relativistic electron plasma. We assemble the transversal and longitudinal tachyonic flux components radiated by the shock-heated electron gas, perform spectral fits to the above mentioned GRBs, and obtain estimates of the tachyonic luminosity and internal energy of the source plasma.

Superluminal wave modes generated by nonlocal electron currents. – The tachyonic radiation field in vacuum is a real vector field with negative mass-square, satisfying the Proca equation $(\Delta-\partial^2/\partial t^2+m_{\rm t}^2)A_\mu=-j_\mu$ [7,8]. $m_{\rm t}$ is the mass of the superluminal Proca field A_μ, and $j_\mu=(-\rho,\mathbf{j})$ the subluminal electron current. Tachyonic radiation implies superluminal signal transfer [9–13], the energy quanta propagating faster than light in vacuum, in contrast to rotating superluminal light sources emitting vacuum Cherenkov radiation [14–16]. Tachyonic wave modes are a kind of photons with negative mass-square, and should not be confused with the apparent superluminal plasma flow of quasar jets due to relativistic beaming [17,18] (whose intrinsic flow speed is safely subluminal), or with superluminal galactic recession velocities in expanding background geometries [19] which are themselves moving in time. The superluminal energy propagation by tachyonic vacuum modes is also to be distinguished from superluminal group velocities arising in photonic crystals, optical fibers, or

(a) E-mail: tom@geminga.org

metamaterials [20–24]. In contrast to tachyonic quanta, the actual signal speed defined by the electromagnetic energy flow in these media is always subluminal and occasionally even opposite to the group velocity.

The Proca equation in Fourier space reads

$$(\Delta + k^2)\hat{A}_0(\mathbf{x},\omega) = \hat{\rho}(\mathbf{x},\omega),\ (\Delta + k^2)\hat{\mathbf{A}} = -\hat{\mathbf{j}}, \quad (1)$$

where $k(\omega) = \sqrt{\omega^2 + m_\mathrm{t}^2}$ is the wave number of the tachyonic modes, subject to the Lorentz condition $\mathrm{i}\omega\hat{A}_0 + \mathrm{div}\,\hat{\mathbf{A}} = 0$. This is equivalent to a set of tachyonic Maxwell equations [7]:

$$\begin{aligned} \mathrm{rot}\,\hat{\mathbf{B}}(\mathbf{x},\omega) + \mathrm{i}\omega\hat{\mathbf{E}}(\mathbf{x},\omega) &= \hat{\mathbf{j}}(\mathbf{x},\omega) + m_\mathrm{t}^2\hat{\mathbf{A}}(\mathbf{x},\omega), \\ \mathrm{div}\,\hat{\mathbf{E}}(\mathbf{x},\omega) &= \hat{\rho}(\mathbf{x},\omega) - m_\mathrm{t}^2\hat{A}_0(\mathbf{x},\omega), \end{aligned} \quad (2)$$

with $\mathrm{rot}\,\hat{\mathbf{E}} - \mathrm{i}\omega\hat{\mathbf{B}} = 0$ and $\mathrm{div}\,\hat{\mathbf{B}} = 0$. The field strengths and potentials are connected by $\hat{\mathbf{E}} = \mathrm{i}\omega\hat{\mathbf{A}} + \nabla\hat{A}_0$ and $\hat{\mathbf{B}} = \mathrm{rot}\,\hat{\mathbf{A}}$. Fourier transforms are defined by $\hat{\mathbf{A}}(\mathbf{x},\omega) = \int_{-\infty}^{+\infty}\mathbf{A}(\mathbf{x},t)\mathrm{e}^{\mathrm{i}\omega t}\mathrm{d}t$.

The charge and current densities of a classical subluminal point particle with trajectory $\mathbf{x}_0(t)$ read $\rho(\mathbf{x},t) = q_\mathrm{t}\delta(\mathbf{x}-\mathbf{x}_0(t))$ and $\mathbf{j}(\mathbf{x},t) = \dot{\mathbf{x}}_0(t)\rho(\mathbf{x},t)$, where q_t is the tachyonic charge carried by the particle. Alternatively, we may consider a Dirac current $j^\mu = (\rho,\mathbf{j}) = -q_t\bar{\psi}\gamma^\mu\psi$ in the field equations, and replace the classical Fourier transforms $(\hat{\rho},\hat{\mathbf{j}})$ by spinorial matrix elements $\hat{\rho}_{mn}(\mathbf{x})$ and $\hat{\mathbf{j}}_{mn}(\mathbf{x})$ [25]. The nonlocal coupling of the superluminal radiation field to the electron current is effected by a frequency-dependent coupling constant $q(\omega)$, which replaces q_t in the Fourier amplitudes. $q(\omega)$ scales with a power of the tachyonic velocity, $q(\omega) = q_\mathrm{t}\upsilon_\mathrm{t}^\sigma$, where $\upsilon_\mathrm{t} = \sqrt{1 + m_\mathrm{t}^2/\omega^2}$, so that q_t is recovered in the high-frequency limit $q(\omega\to\infty) = q_\mathrm{t}$. The varying tachyonic fine-structure constant thus reads

$$\alpha_\mathrm{q}(\omega) = \frac{q^2(\omega)}{4\pi\hbar c} = \alpha_\mathrm{t}\hat{\Omega}^2(\omega), \quad \hat{\Omega}(\omega) := \left(1 + \frac{m_\mathrm{t}^2}{\omega^2}\right)^{\sigma/2}. \quad (3)$$

The frequency dependence of $\alpha_\mathrm{q}(\omega)$ is weak at high energy $\omega \gg m_\mathrm{t}$, but it shows in the soft γ-ray band relevant for GRB spectra [1–5]. In the low-frequency regime, we find $\alpha_\mathrm{q}(\omega\to 0) \propto \omega^{-2\sigma}$, and the constant $\alpha_\mathrm{t} = q_\mathrm{t}^2/(4\pi\hbar c)$ is recovered at high frequencies, $\alpha_\mathrm{q}(\infty) = \alpha_\mathrm{t}$. The nonlocal charge and current densities depending on the varying coupling constant $q(\omega) = q_\mathrm{t}\hat{\Omega}(\omega)$ are denoted by a subscript Ω, $\hat{\rho}_\Omega(\mathbf{x},\omega) = \hat{\Omega}(\omega)\hat{\rho}(\mathbf{x},\omega)$, and $\hat{\mathbf{j}}_\Omega = \hat{\Omega}(\omega)\hat{\mathbf{j}}$, with $\hat{\Omega}(\omega)$ in (3).

The dispersion of the charge and current densities induced by the varying coupling constant becomes apparent in real time,

$$\rho_\Omega(\mathbf{x},t) = \frac{1}{2\pi}\int_{-\infty}^{\infty}\hat{\rho}_\Omega(\mathbf{x},\omega)\mathrm{e}^{-\mathrm{i}\omega t}\mathrm{d}\omega = \int_{-\infty}^{\infty}\Omega(t')\rho(\mathbf{x},t-t')\mathrm{d}t', \quad (4)$$

and analogously for the current $\mathbf{j}_\Omega$, where

$$\Omega(t) = \delta(t) + \Omega_\mathrm{reg}(t), \quad \Omega_\mathrm{reg}(t) = \frac{1}{2\pi}\int_{-\infty}^{\infty}\hat{\Omega}_\mathrm{reg}(\omega)\mathrm{e}^{-\mathrm{i}\omega t}\mathrm{d}\omega, \quad (5)$$

so that $\hat{\Omega}_\mathrm{reg}(\omega) = \hat{\Omega}(\omega) - 1$, and $\delta(t)$ is the Dirac function. The integral (5) converges for scaling exponents $\sigma < 1$, cf. (3), which we henceforth assume. $\Omega_\mathrm{reg}(t)$ is symmetric in t, admitting power law decay $\Omega_\mathrm{reg}(t) \propto |t|^{\sigma-1}$ for $m_\mathrm{t}|t| \to \infty$. This power law tail of $\Omega(t)$ generates the long-range dispersion of the charge and current densities (4). Only at negative even integer σ, the decay is exponential $\propto \mathrm{e}^{-m_\mathrm{t}|t|}$ and the dispersion localized. The relevant interval for GRBs is $0 < \sigma < 1$, where $\Omega_\mathrm{reg}(t)$ is positive and monotonically decaying.

Tachyonic spectral functions of GRB plasmas. – The quantized tachyonic radiation densities of an inertial spinning charge read [26]

$$p^{\mathrm{T,L}}(\omega,\gamma) = m_\mathrm{t}^2\frac{\alpha_\mathrm{q}(\omega)\omega}{\omega^2 + m_\mathrm{t}^2}\left[\gamma^2 - \frac{m_\mathrm{t}}{m}\frac{\omega}{m_\mathrm{t}}\gamma - \frac{1}{4}\frac{m_\mathrm{t}^2}{m^2} - \left(1 + \frac{\omega^2}{m_\mathrm{t}^2}\right)\Delta^{\mathrm{T,L}}\right]\frac{1}{\gamma\sqrt{\gamma^2-1}}, \quad (6)$$

where the superscripts T and L refer to the transversal/longitudinal polarization components defined by $\Delta^\mathrm{T} = 1 - m_\mathrm{t}^2/(2m^2)$ and $\Delta^\mathrm{L} = 0$. m and γ denote mass and Lorentz factor of the electron, m_t is the tachyon mass and $\alpha_\mathrm{q}(\omega) = \alpha_\mathrm{t}\hat{\Omega}^2(\omega)$ the varying tachyonic fine-structure constant (3).

The spectral functions of the electron plasma are calculated by averaging the tachyonic radiation densities with a thermal or nonthermal electronic power law distribution [13],

$$B^{\mathrm{T,L}}(\omega,\gamma_1) = \frac{1}{\alpha_\mathrm{t}}\int_{\gamma_1}^{\infty}p^{\mathrm{T,L}}(\omega,\gamma)\mathrm{d}\hat{\rho}_{\alpha,\beta}(\gamma). \quad (7)$$

The normalization factor $A_{\alpha,\beta}$ of the electron density $\mathrm{d}\hat{\rho}_{\alpha,\beta} = \gamma^{-\alpha-1}\mathrm{e}^{-\beta\gamma}\sqrt{\gamma^2-1}\mathrm{d}\gamma$ is related to the electron count by $n_\mathrm{e} = A_{\alpha,\beta}K_{\alpha,\beta}$, where $K_{\alpha,\beta} = \int_1^\infty \mathrm{d}\hat{\rho}_{\alpha,\beta}(\gamma)$. The electron temperature can be inferred from the exponential cutoff, $\beta = m/(kT)$ or $kT[\mathrm{keV}] \approx 511/\beta$. We consider ultra-relativistic multi-component plasmas in the collisionless regime [27], in stationary non-equilibrium described by power law densities [28,29].

The averaged radiation densities read

$$\langle p^{\mathrm{T,L}}(\omega)\rangle_{\alpha,\beta} = A_{\alpha,\beta}\alpha_\mathrm{t}B^{\mathrm{T,L}}(\omega,\hat{\gamma}(\omega)), \quad (8)$$

where

$$\hat{\gamma}(\omega) = \mu_\mathrm{t}\sqrt{1 + \frac{\omega^2}{m_\mathrm{t}^2}} + \frac{1}{2}\frac{\omega}{m}, \quad \mu_\mathrm{t} = \sqrt{1 + \frac{1}{4}\frac{m_\mathrm{t}^2}{m^2}}. \quad (9)$$

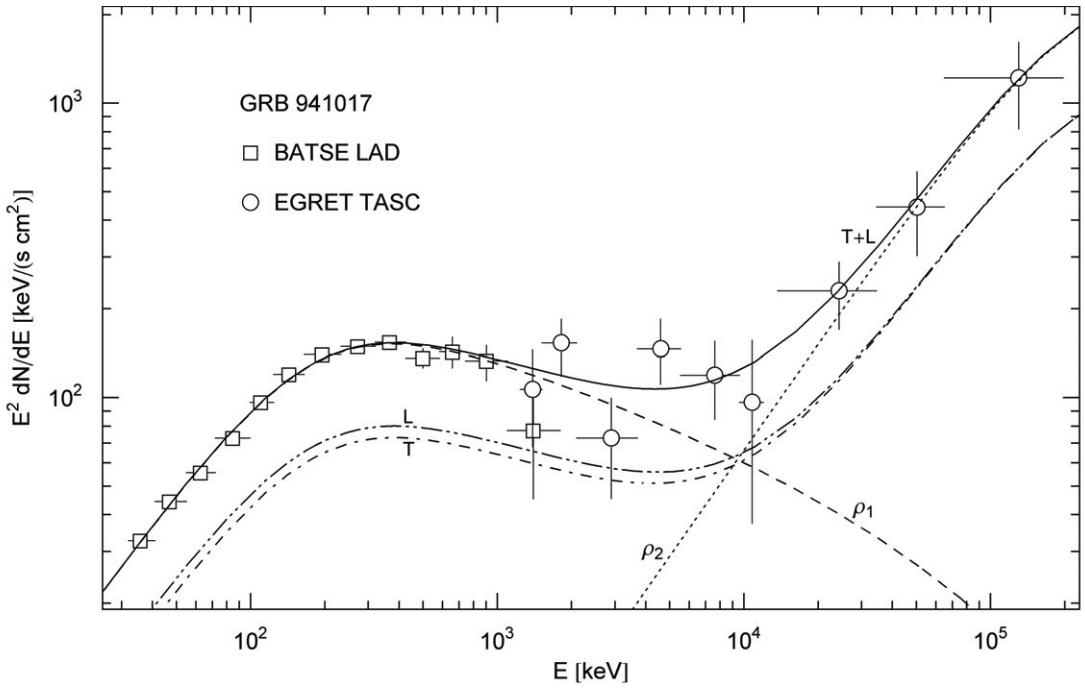

Fig. 1: Spectral map of γ-ray burst GRB 941017. BATSE and EGRET data points from ref. [4]. The solid line T + L depicts the unpolarized differential tachyon flux $\mathrm{d}N^{\mathrm{T+L}}/\mathrm{d}E$, obtained by adding the flux densities $\rho_{1,2}$ radiated by an ultra-relativistic two-component plasma, cf. (12). The transversal and longitudinal densities add up to the total unpolarized flux, $\mathrm{T+L} = \rho_1 + \rho_2$. The nonthermal low-energy flux ρ_1 is fitted with the tachyon-electron mass ratio $m_\mathrm{t}/m \approx 0.37$, cf. table 1; the exponential decay of this flux component sets in at about $E_\mathrm{cut} \approx 0.75\,\mathrm{GeV}$, cf. after (14). The mass ratio $m_\mathrm{t}/m \approx 430$ and the cutoff energy $E_\mathrm{cut} \approx 21\,\mathrm{GeV}$ of the thermal high-energy component ρ_2 are tentative, owing to lack of flux data above 100 MeV.

The spectral functions can be reduced to incomplete gamma functions,

$$B^{\mathrm{T,L}}(\omega,\gamma_1) = m_\mathrm{t}\hat{\omega}^{1-2\sigma}(1+\hat{\omega}^2)^{\sigma-1}\left[b_3 - \frac{m_\mathrm{t}}{m}\hat{\omega}b_2 - \left(\frac{1}{4}\frac{m_\mathrm{t}^2}{m^2} + (1+\hat{\omega}^2)\Delta^{\mathrm{T,L}}\right)b_1\right], \quad (10)$$

with $\Delta^{\mathrm{T,L}}$ as in (6), $\hat{\omega} = \omega/m_\mathrm{t}$, and $b_k = \beta^{\alpha+2-k}\Gamma(k-\alpha-2, \beta\gamma_1)$. The unpolarized density $\langle p^{\mathrm{T+L}}(\omega)\rangle_{\alpha,\beta}$ is obtained by adding the polarization components. In the following, we use keV units for the tachyon and electron mass and the radiated frequency, so that ω stands for $\hbar\omega[\mathrm{keV}]$ and m_t for $m_\mathrm{t}c^2[\mathrm{keV}]$; $B^{\mathrm{T,L}}$ and $\langle p^{\mathrm{T,L}}(\omega)\rangle_{\alpha,\beta}$ are meant in keV units as well. The spectral functions (10) decay exponentially for $\beta\gamma_1 \gg 1$, since $\Gamma \propto \mathrm{e}^{-\beta\gamma_1}$, and so does $B^{\mathrm{T,L}}(\omega, \hat{\gamma}(\omega))$ for $\hat{\omega} \to \infty$. We define the cutoff frequency as $\hat{\gamma}(\omega_\mathrm{cut}) - \hat{\gamma}(0) = 1/\beta$ or $\omega_\mathrm{cut} = \omega_\mathrm{max}(\mu_\mathrm{t} + 1/\beta)$, where [6]

$$\omega_\mathrm{max}(\gamma) = m_\mathrm{t}\left(\mu_\mathrm{t}\sqrt{\gamma^2-1} - \frac{1}{2}\frac{m_\mathrm{t}}{m}\gamma\right). \quad (11)$$

The low-frequency scaling of the averaged spectral density (8) is $\langle p^{\mathrm{T,L}}\rangle_{\alpha,\beta} \propto \alpha_\mathrm{q}(\omega)\omega \sim \omega^{1-2\sigma}$, valid for $\omega \ll m_\mathrm{t}$. Typical values of the electron index range in $-2 \leqslant \alpha \leqslant 2$, and the fine-structure scaling exponent σ is usually close to 0.5 for GRBs [3,4]. In the intermediate regime $m_\mathrm{t} \ll \omega \ll \omega_\mathrm{cut}$, we find $\langle p^{\mathrm{T,L}}\rangle_{\alpha,\beta} \propto \omega^{-\alpha}$ for $\alpha > 1$, and $\langle p^{\mathrm{T,L}}\rangle_{\alpha,\beta} \propto 1/\omega$ if $\alpha \leqslant 1$. This power law scaling in the high-temperature regime is only approximately realized, so that the crossover is not a straight power law slope, but slightly curved in double-logarithmic plots, gradually bending into exponential decay setting in at ω_cut. $\langle p^{\mathrm{T,L}}\rangle_{\alpha,\beta}$ is peaked at the junction $\omega \approx m_\mathrm{t}$ of the two power law slopes. If $\omega_\mathrm{cut} < m_\mathrm{t}$, which can occur in the low-temperature regime [8], the low-frequency power law is exponentially cut at ω_cut without power law crossover, and $\langle p^{\mathrm{T,L}}\rangle_{\alpha,\beta}$ peaks in the vicinity of ω_cut.

Flux densities in the soft γ-ray band: Spectral fits of GRB 941017, GRB 990123, and GRB 990104. – The spectral fits in figs. 1–3 are based on the E^2-rescaled differential flux densities

$$E^2\frac{\mathrm{d}N^{\mathrm{T,L}}}{\mathrm{d}E}[\mathrm{keV\,cm^{-2}\,s^{-1}}] = \omega[\mathrm{keV}]\frac{\langle p^{\mathrm{T,L}}(\omega)\rangle_{\alpha,\beta}[\mathrm{keV}]}{4\pi d^2[\mathrm{cm}]\hbar[\mathrm{keV\,s}]}, \quad (12)$$

where $E = \hbar\omega$ is the energy of the radiated tachyons, $\langle p^{\mathrm{T,L}}(\omega)\rangle_{\alpha,\beta}$ the spectral average (8), d the distance to the source, and $\hbar[\mathrm{keV\,s}] \approx 6.582 \times 10^{-19}$. We substitute the radiation density (8), and replace $A_{\alpha,\beta}\alpha_\mathrm{t}/d^2$ by a single parameter $\hat{n}$ determining the flux amplitude,

$$\frac{\hat{n}[\mathrm{keV\,cm^{-2}\,s^{-1}}]}{K_{\alpha,\beta}m_\mathrm{t}^2[\mathrm{keV}]} = \frac{A_{\alpha,\beta}\alpha_\mathrm{t}}{4\pi d^2[\mathrm{cm}]\hbar[\mathrm{keV\,s}]} \approx 1.270 \times 10^{-32}\frac{A_{\alpha,\beta}\alpha_\mathrm{t}}{d^2[\mathrm{Mpc}]}, \quad (13)$$

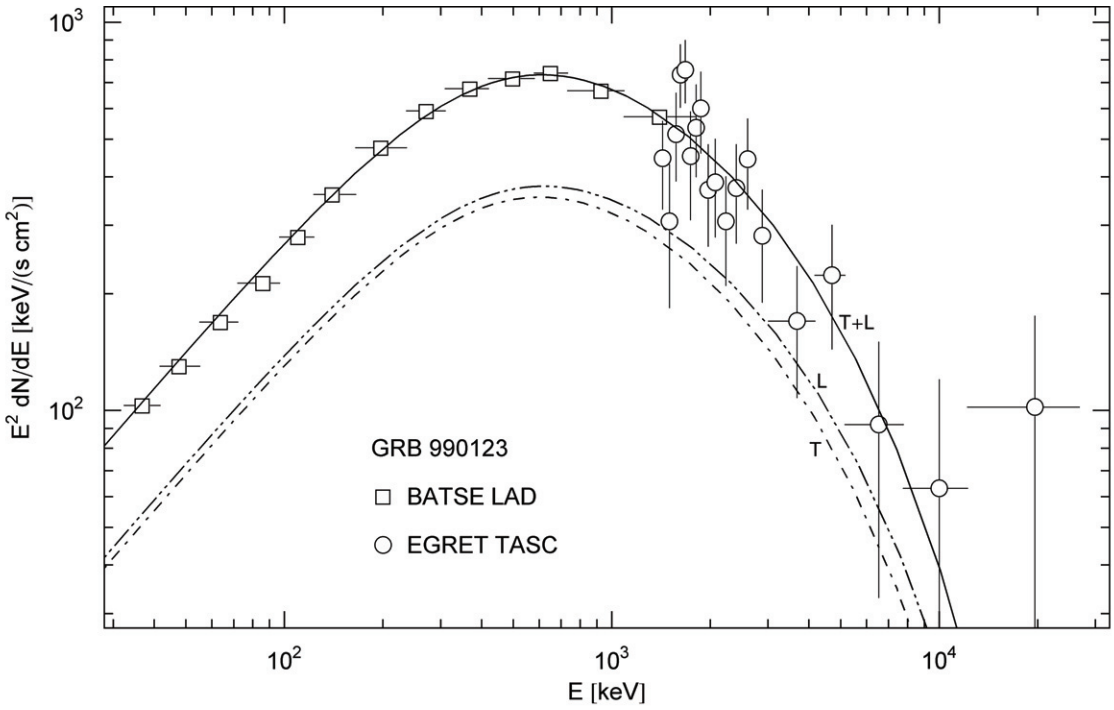

Fig. 2: Spectral map of GRB 990123. Flux data from ref. [4]. T and L stand for the transversal and longitudinal flux components, and $\mathrm{T}+\mathrm{L}=\rho_1$ labels the unpolarized flux generated by a one-component plasma. The tachyon-electron mass ratio is $m_\mathrm{t}/m\approx 0.92$, and the tachyonic flux density $\mathrm{T}+\mathrm{L}$ is exponentially cut at $E_\mathrm{cut}\approx 5.4\,\mathrm{MeV}$. The least-squares fit is performed with the unpolarized flux, and subsequently split into transversal and longitudinal components. The parameters of the nonthermal electronic source plasma are recorded in tables 1 and 2.

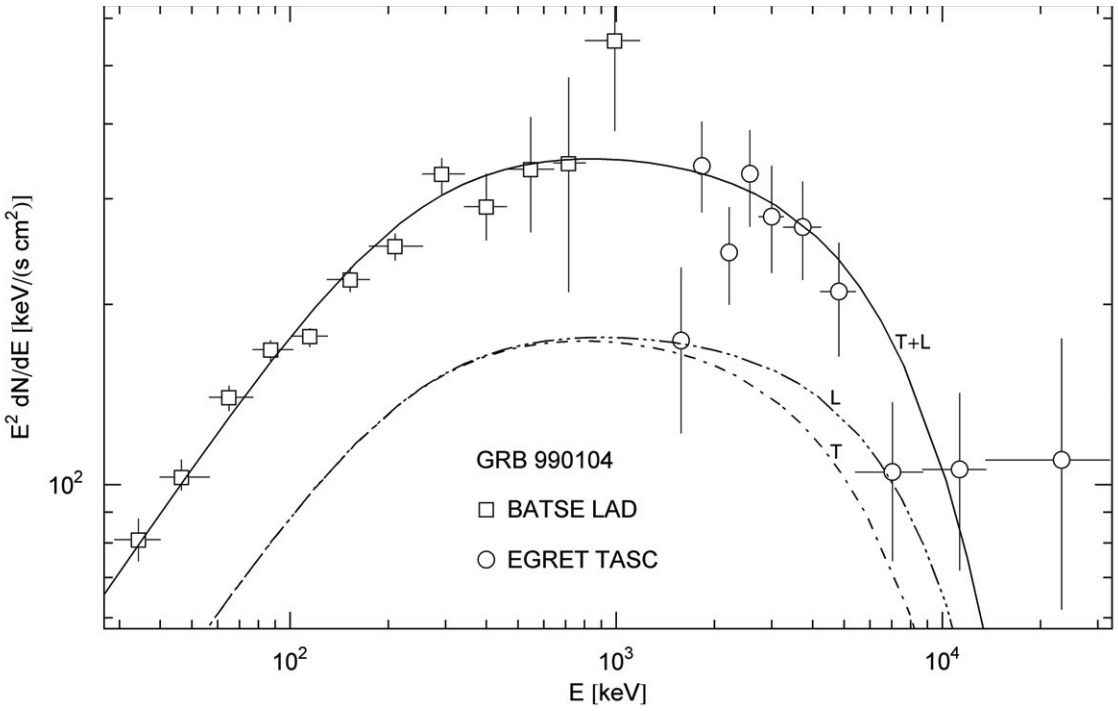

Fig. 3: Spectral map of GRB 990104. Data points from ref. [4], notation as in figs. 1 and 2. The superluminal flux is radiated by a thermal single-component electron plasma, cf. table 1. The cutoff energy of the tachyonic flux density $\rho_1=\mathrm{T}+\mathrm{L}$ is $E_\mathrm{cut}\approx 3.8\,\mathrm{MeV}$, and the tachyon-electron mass ratio is $m_\mathrm{t}/m\approx 0.47$.

Table 1: Electron distributions ρ_i generating the tachyonic flux densities of the γ-ray bursts in figs. 1–3. The components $\rho_{1,2}$ of the source plasma are specified by electronic power law densities with electron index α and cutoff parameter β in the Boltzmann factor, cf. after (7). m_t is the mass parameter of the superluminal modes, and σ the scaling exponent of the frequency-dependent tachyonic fine-structure constant (3). The scale factor $\hat{n}$ determining the amplitude of the superluminal flux and the electron number is defined in (13). kT is the temperature of the thermal ($\alpha = -2$) or nonthermal plasma components.

GRB	m_t (keV)	σ	α	β	$\hat{n}$ (keV cm^{-2} s^{-1})	kT (MeV)
941017						
ρ_1	190	0.42	1.2	2.11×10^{-4}	116	2.42×10^3
ρ_2	2.2×10^5	0.4	-2	2.44×10^{-5}	1.36×10^3	2.09×10^4
990123						
ρ_1	470	0.5	0.6	5.88×10^{-2}	689	8.69
990104						
ρ_1	240	0.6	-2	5.33×10^{-2}	190	9.59

Table 2: Tachyonic luminosity, electron count, and internal energy of the source plasma. $\langle P^{\mathrm{T,L}}\rangle_{\alpha,\beta}$ denotes the power transversally and longitudinally radiated, cf. (16). α_t is the tachyonic fine-structure constant in the high-frequency limit, cf. (18), estimated from the burst duration τ_0 [4]. n_e is the electron number (14), and U the internal energy (17) of the respective plasma component ρ_i, cf. table 1. The tachyonic power, electron number, and the energy stored in the electron gas scale $\propto z^2$; we list these quantities at $z = 1$, since a redshift estimate is only available for GRB 990123, $z \approx 1.6$ [30].

GRB	τ_0 (s)	$\langle P^\mathrm{T}\rangle_{\alpha,\beta}/z^2$ (erg/s)	$\langle P^\mathrm{L}\rangle_{\alpha,\beta}/z^2$ (erg/s)	α_t	n_e/z^2	U/z^2 (erg)
941017	262.1					
ρ_1		1.26×10^{51}	1.41×10^{51}	1.24×10^{-21}	3.96×10^{57}	6.98×10^{53}
ρ_2		2.64×10^{52}	2.51×10^{52}	3.19×10^{-25}	1.35×10^{56}	1.35×10^{55}
990123	98.4					
ρ_1		4.19×10^{51}	4.55×10^{51}	3.10×10^{-23}	1.54×10^{59}	8.60×10^{53}
990104	262.2					
ρ_1		2.82×10^{51}	3.02×10^{51}	1.52×10^{-22}	3.33×10^{58}	1.53×10^{54}

where $d[\mathrm{cm}] \approx 3.086 \times 10^{24} d[\mathrm{Mpc}]$. The burst distance is estimated via $d \sim cz/H_0$, with the Hubble distance $c/H_0 \approx 4.41\,\mathrm{Gpc}$ ($h_0 \approx 0.68$). Thus, $d[\mathrm{Gpc}] \approx 4.41\,z$, and we calculate the electron number of the source plasma as, cf. after (7),

$$n_\mathrm{e} = A_{\alpha,\beta} K_{\alpha,\beta} \approx 1.53 \times 10^{39} \frac{\hat{n}[\mathrm{keV\,cm^{-2}\,s^{-1}}]}{\alpha_\mathrm{t} m_\mathrm{t}^2[\mathrm{keV}]} z^2. \quad (14)$$

The asymptotic energy scaling of the flux densities (12) is $E^2 \mathrm{d}N^{\mathrm{T,L}}/\mathrm{d}E \propto E^{2(1-\sigma)}$, applicable for $E/m_\mathrm{t} \ll 1$, cf. after (11). In the crossover region $m_\mathrm{t} \ll E \ll E_\mathrm{cut}$, we find in leading order $E^2 \mathrm{d}N^{\mathrm{T,L}}/\mathrm{d}E \propto E^{1-\alpha}$ if $\alpha > 1$, and $E^2 \mathrm{d}N^{\mathrm{T,L}}/\mathrm{d}E \propto 1$ for $\alpha \leqslant 1$, which terminates in exponential decay at $E_\mathrm{cut} = \hbar\omega_\mathrm{max}(1/\beta + \mu_\mathrm{t})$.

The spectral fits are performed with the unpolarized flux density $\mathrm{d}N^{\mathrm{T+L}} = \mathrm{d}N^\mathrm{T} + \mathrm{d}N^\mathrm{L}$ (denoted by T + L in figs. 1–3) of the plasma components ρ_i specified by electronic power law distributions in table 1. The corresponding tachyonic flux components are likewise denoted by ρ_i, cf. fig. 1, and add up to the total unpolarized flux $\mathrm{T} + \mathrm{L} = \sum \rho_i$. Different plasma components ρ_i radiate tachyons with different mass-square. The tachyon mass extracted from the spectral fits of GRB 990123 in fig. 2 and GRB 990104 in fig. 3, as well as from the low-energy component ρ_1 of GRB 941017 in fig. 1 is comparable to the electron mass, cf. table 1. A notably larger tachyon-electron mass ratio is inferred from the high-energy flux component ρ_2 of GRB 941017, cf. the caption to fig. 1.

The transversal/longitudinal tachyonic luminosity $\langle P^{\mathrm{T,L}}\rangle_{\alpha,\beta}$ of the source plasma is obtained by a frequency integration of the averaged spectral densities $\langle p^{\mathrm{T,L}}(\omega)\rangle_{\alpha,\beta}$,

$$\langle P^{\mathrm{T,L}}\rangle_{\alpha,\beta}[\mathrm{keV/s}] = \frac{1}{\hbar[\mathrm{keV\,s}]} \int_0^\infty \langle p^{\mathrm{T,L}}(\omega)\rangle_{\alpha,\beta}[\mathrm{keV}]\mathrm{d}\omega[\mathrm{keV}]. \quad (15)$$

The integrand decays exponentially at high frequencies; convergence at the lower integration boundary requires $\sigma < 1$, cf. after (11). On substituting (8) into (15), and making use of (13), we obtain

$$\langle P^{\mathrm{T,L}}\rangle_{\alpha,\beta}[\mathrm{keV/s}] = \frac{4\pi d^2[\mathrm{cm}]\hat{n}}{K_{\alpha,\beta} m_\mathrm{t}^2[\mathrm{keV}]} \int_0^\infty B^{\mathrm{T,L}}(\omega, \hat{\gamma}(\omega))\mathrm{d}\omega. \quad (16)$$

Conversion into erg/s units means to multiply by 1.602×10^{-9}. $\hat{n}$ is the tachyonic flux amplitude in units of keV cm^{-2} s^{-1}, and $4\pi d^2[\mathrm{cm}] \approx 2.33 \times 10^{57}\, z^2$, cf. after (13). The redshift estimate of GRB 990123 in fig. 2 is $z \approx 1.6$ [30], which amounts to 7 Gpc. The high-energy component ρ_2 of GRB 941017 in fig. 1 does not imply

a low redshift, as there is no intergalactic absorption of the tachyon flux. Tachyonic γ-rays are not attenuated by cosmic background photons, as tachyons and photons can only indirectly interact via matter fields [28,29,31].

The high-temperature limit ($\beta\to 0$) of the internal energy $U=n_{\rm e}mc^2u_\alpha(\beta)$ of the ultra-relativistic electron gas defined by density $\mathrm{d}\hat\rho_{\alpha,\beta}$, cf. after (7), reads [32]

$$u_{\alpha<1}\sim\frac{1-\alpha}{\beta},\quad u_{1<\alpha<2}\sim\frac{2\alpha}{\sqrt{\pi}}\frac{\Gamma(\alpha/2)\Gamma(2-\alpha)}{\Gamma((\alpha-1)/2)}\beta^{\alpha-2}. \quad (17)$$

The electron energy of each plasma component ρ_i is recorded in table 2, with $mc^2\approx 8.187\times 10^{-7}\,\mathrm{erg}$. We identify the time scale $\tau_0=U/\langle P^{\mathrm{T+L}}\rangle_{\alpha,\beta}$ with the burst duration, typically of the order of 100 s, in which the internal energy of the electron gas is radiated off. We use $U[\mathrm{keV}]=n_{\rm e}m[\mathrm{keV}]u_\alpha(\beta)$ and $\langle P^{\mathrm{T+L}}\rangle_{\alpha,\beta}$ in (16) with $4\pi d^2\hat n=n_{\rm e}\alpha_{\rm t}m_{\rm t}^2/\hbar$, cf. (13), to estimate the asymptotic fine-structure constant from the burst duration,

$$\alpha_{\rm t}=\frac{m[\mathrm{keV}]\hbar[\mathrm{keV\,s}]K_{\alpha,\beta}u_\alpha(\beta)}{\tau_0[\mathrm{s}]\int_0^\infty B^{\mathrm{T+L}}(\omega,\hat\gamma(\omega))\mathrm{d}\omega}. \quad (18)$$

Once $\alpha_{\rm t}$ is known, we can calculate the electron number and internal energy of the plasma, as well as the tachyonic power radiated, cf. table 2.

Conclusion. – We discussed the coupling of superluminal radiation fields to a plasma current by a frequency-dependent fine-structure constant (3), resulting in a nonlocal interaction of the tachyonic modes with the GRB plasma. We studied tachyonic radiation densities subject to an energy-dependent coupling constant, and explained the spectral averaging over the plasma components constituting the GRBs. The low-frequency scaling of the averaged spectral densities (8) is determined by the scaling exponent of the tachyonic fine-structure constant. The high-frequency crossover between the spectral peak and exponential cutoff depends on the electronic power law index of the plasma, cf. after (11).

The averaged radiation densities (8) were put to test by performing tachyonic spectral fits to burst spectra in the soft γ-ray band, cf. figs. 1–3. We showed that the low-energy components as well as the occasionally observed high-energy slopes of GRB spectra can be fitted with tachyonic flux densities. The fits are based on the tachyonic radiation densities (6) averaged over electronic power law distributions, cf. after (7); no additional radiation mechanism is invoked for the high-energy component of GRB 941017 in fig. 1. The spectral fitting of GRBs described here does not require any detailed modeling of the burst evolution, no specific assumptions on the progenitor and heating mechanism, not even a distance estimate; only the inferred tachyonic power, the electron number, and internal energy of the source plasma scale with redshift.

The mass of the radiated quanta and the scaling exponent of the tachyonic fine-structure constant $\alpha_{\rm q}(\omega)=\alpha_{\rm t}v_{\rm t}^{2\sigma}$ depend on the respective plasma component ρ_i generating the tachyon flux, and can be extracted from the spectral fit, cf. table 1; the scaling amplitude $\alpha_{\rm t}=\alpha_{\rm q}(\omega\to\infty)$ is estimated from the burst duration. The superluminal velocity $v_{\rm t}$ coincides with the vacuum refractive index $k/\omega=\sqrt{1+m_{\rm t}^2/\omega^2}$ [31]. It is possible that $\alpha_{\rm t}$ scales with the tachyon-electron mass ratio, $\alpha_{\rm t}=\alpha_0(m_{\rm t}/m)^{-2\sigma}$, with a universal amplitude α_0 of the order of 10^{-22}, but the spectral fits in figs. 1–3 do not yet allow a definite conclusion on that. The constituents of a multi-component source plasma can be disentangled by identifying the corresponding flux components ρ_i in the spectral maps, as done in the case of GRB 941017, cf. fig. 1. The tachyonic luminosity of each plasma component is listed in table 2.

REFERENCES

[1] Racusin J. L. *et al.*, *Nature*, **455** (2008) 183.
[2] Sugita S. *et al.*, *AIP Conf. Proc.*, **1000** (2008) 354.
[3] Wigger C. *et al.*, *Astrophys. J.*, **675** (2008) 553.
[4] Kaneko Y. *et al.*, *Astrophys. J.*, **677** (2008) 1168.
[5] Abdo A. A. *et al.*, *Science*, **323** (2009) 1688.
[6] Tomaschitz R., *EPL*, **85** (2009) 29001.
[7] Tomaschitz R., *Opt. Commun.*, **282** (2009) 1710.
[8] Tomaschitz R., *Physica B*, **405** (2010) 1022.
[9] Tanaka S., *Prog. Theor. Phys.*, **24** (1960) 171.
[10] Feinberg G., *Sci. Am.*, **222** (2) (1970) 69.
[11] Tomaschitz R., *Astropart. Phys.*, **27** (2007) 92.
[12] Tomaschitz R., *Phys. Lett. A*, **366** (2007) 289.
[13] Tomaschitz R., *Physica A*, **387** (2008) 3480.
[14] Bolotovskiĭ B. M. and Serov A. V., *Phys.-Usp.*, **48** (2005) 903.
[15] Bessarab A. V. *et al.*, *IEEE Trans. Plasma Sci.*, **32** (2004) 1400.
[16] Bessarab A. V. *et al.*, *Radiat. Phys. Chem.*, **75** (2006) 825.
[17] Kellermann K. I. *et al.*, *Astrophys. Space Sci.*, **311** (2007) 231.
[18] Jester S., *Mon. Not. R. Astron. Soc.*, **389** (2008) 1507.
[19] Davis T. M. and Lineweaver C. H., *Publ. Astron. Soc. Australia*, **21** (2004) 97.
[20] Bigelow M. S., Lepeshkin N. N. and Boyd R. W., *Science*, **301** (2003) 200.
[21] Baba T., *Nat. Photon.*, **2** (2008) 465.
[22] Gehring G. M. *et al.*, *Science*, **312** (2006) 895.
[23] Thévenaz L., *Nat. Photon.*, **2** (2008) 474.
[24] Dolling G. *et al.*, *Science*, **312** (2006) 892.
[25] Tomaschitz R., *Eur. Phys. J. D*, **32** (2005) 241.
[26] Tomaschitz R., *Ann. Phys. (N.Y.)*, **322** (2007) 677.
[27] Minguzzi A. and Tosi M. P., *Physica B*, **300** (2001) 27.
[28] Tomaschitz R., *EPL*, **84** (2008) 19001.
[29] Tomaschitz R., *Phys. Lett. A*, **372** (2008) 4344.
[30] Andersen M. I. *et al.*, *Science*, **283** (1999) 2075.
[31] Tomaschitz R., *Physica B*, **404** (2009) 1383.
[32] Tomaschitz R., *Physica A*, **385** (2007) 558.